First-order character of the smectic-*A* to chiral nematic transition in chiral liquid-crystal mixtures

P. Jamée, G. Pitsi, and J. Thoen
Laboratorium voor Akoestiek en Thermische Fysica, Departement Natuurkunde en Sterrenkunde, Katholieke Universiteit Leuven, Celestijnenlaan 200D, B-3001 Leuven, Belgium

(Received 3 December 2002; published 20 March 2003)

An investigation into the smectic-*A* to chiral nematic ($N'A$) transition in liquid crystals is presented by using adiabatic scanning calorimetry (ASC). It is predicted theoretically that chirality drives this transition to first order. This transition is studied in mixtures of the nonchiral liquid crystal octyloxycyanobiphenyl (8OCB) and the chiral 4-(2-methylbutyl)-4′-cyanobiphenyl (CB15), a system with a large (chiral) nematic region that widens upon increasing the chiral (CB15) fraction. An ASC measurement on pure 8OCB showed no evidence for a latent heat, in agreement with previous ac calorimetric studies, with an upper boundary for the latent heat (if any) of 1.8 J/kg. Since pure 8OCB has no measurable latent heat, and taking into account the widening of the chiral nematic region, the possibility of a continuous to first-order crossover due to the coupling of the nematic and the smectic order parameters, as occurring in several cases of smectic-*A* to nematic (*NA*) transitions, can be excluded. However, for all examined mixtures a latent heat could be determined at the smectic-*A* to chiral nematic transition. This confirms theoretical predictions of the first order character of this transition. Quantitatively, theoretical predictions of the evolution of the entropy discontinuities and latent heats of this transition were not consistent with the experimental results. It was further observed that the transition temperature decreases linearly in agreement with theoretical predictions and a previous ac calorimetric study. Finally, it was observed that the pretransitional specific heat capacity shows an interesting evolution upon increasing chiral fraction, and it may be concluded that any theoretical model based on Landau theory is not sufficient to describe this transition.

DOI: 10.1103/PhysRevE.67.031703 PACS number(s): 61.30.−v, 64.70.Md

I. INTRODUCTION

Liquid crystals exhibit one or more mesophases located between the solid and the isotropic liquid states and having a symmetry intermediate to liquids and that of crystals. A wide variety of such liquid crystalline phases can be found, possessing orientational order but having no or reduced positional order [1,2].

In this field of research, the transition between the smectic-*A* (Sm*A*) and the nematic (*N*) phase in (nonchiral) liquid crystals has been the subject of intensive study, both theoretically and experimentally [3]. It has been shown by de Gennes [1,4] that the strength of the coupling between the smectic and the nematic order parameter affects the order of the smectic-*A* to nematic transition. Strong coupling, which corresponds with narrow nematic ranges, results in a first order transition, while weak coupling, associated with a large nematic width, should give continuous transitions. Adiabatic scanning calorimetry (ASC) measurements on the mixtures of 9CB+10CB [5] and of 8CB+10CB (CB, cyanobiphenyl) [6] are consistent with this picture. However, it was predicted by Halperin, Lubensky, and Ma [7] that fluctuations may drive a continuous transition to first order when two interacting order parameters are present, and that consequently the *NA* transition is (very) weakly first order. Recently a study using a high-resolution real-space optical technique showed quantitative evidence for the presence of a small (about 2 mK) two-phase region and a smectic order parameter discontinuity for the *NA* transition in 8CB [8].

It is now well established that (calamitic) chiral liquid crystals can exhibit a number of phases, such as chiral nematic (N^*), chiral smectic-*C* (SmC^*), twist-grain-boundary (TGB), and blue phases (BPs), which a nonchiral compound cannot [9,10]. It is suggested theoretically [11,12] that chirality always drives the smectic-*A* to chiral nematic (N^*A) transition first order. If indeed this is the case, and if one would like to test this, one would like to rule out any possibility of a crossover effect similar to that of the *NA* transition. In order to distinguish both effects, one thus has to make sure that the chiral nematic width is sufficient. Furthermore, it would be interesting to study the influence of changing overall chirality on the latent heat of the N^*A transition, if present.

This can be accomplished by investigating mixtures of a nonchiral compound—exhibiting an *NA* transition—and a chiral compound—chosen such that an N^*A transition is present in these mixtures. In this manner, by varying the amount of the chiral compound, mixtures with varying overall chirality are obtained. In order to rule out any continuous to first order crossover not associated with chirality, two requirements have to be fulfilled. First, the *NA* transition in the pure nonchiral compound has to be continuous, i.e., the nematic width has to be sufficiently large. Second, upon addition of the chiral compound, the chiral nematic width should increase, so one can be sure that no increase in coupling of the smectic and nematic order parameters occurs.

Therefore we have investigated mixtures of the nonchiral liquid crystal octyloxycyanobiphenyl (8OCB) and the chiral 4-(2-methylbutyl)-4′-cyanobiphenyl (CB15). Investigations of pure 8OCB using the ac calorimetric technique show no evidence for a coexistence region at the *NA* transition [13,14], which is not surprising in view of the large nematic width of about 13 K. As was pointed out by Hwang *et al.* [15], mixtures with CB15 result in an N^*A transition with an

increasingly large chiral nematic width upon increasing the weight fraction of CB15. The *NA* transition in pure 8OCB was closely examined in order to investigate whether or not evidence could be found in this compound of the Halperin-Lubensky-Ma effect [7] predicting a first-order *NA* transition. By employing ASC values were further obtained for the evolution of transition temperatures, latent heats, as well as effects on the pretransitional specific heat capacity as a function of an increasing chiral CB15 fraction. This is compared with theoretical approaches as proposed in Refs. [12,11].

II. THEORETICAL BACKGROUND

A. The Lubensky model

In 1975, Lubensky [11] proposed a theoretical model of the smectic-*A* to chiral nematic transition based on an analogy with superconductors following the groundbreaking work of de Gennes [1]. This model will be sumarized here.

The free energy F_n of a smectic-*A* liquid crystal, with layer spacing d is equal to

$$F_n = a|\Psi|^2 + \frac{b}{2}|\Psi|^4 + \gamma_{\|}|\nabla_{\|}\Psi|^2 + \gamma_{\perp}|(\nabla_{\perp} - iq_s\delta\mathbf{n})\Psi|^2 + \frac{K_1}{2}(\boldsymbol{\nabla}\cdot\mathbf{n})^2 + \frac{K_2}{2}(\mathbf{n}\cdot(\boldsymbol{\nabla}\times\mathbf{n}))^2 + \frac{K_3}{2}(\mathbf{n}\times(\boldsymbol{\nabla}\times\mathbf{n}))^2, \tag{1}$$

where $\|$, $\perp$ refer, respectively, to the variations parallel and perpendicular to the director $\mathbf{n}$; d is the smectic layer spacing; $q_s = 2\pi/d$; K_1, K_2, and K_3 are the Frank elastic constants; and $a = a_0(T - T_{NA})$ with a_0 a positive constant and T_{NA} the smectic-*A* to nematic transition temperature.

For the transition from the smectic-*A* to a chiral nematic phase, a cholesteric twist term is added to the free energy *G*, giving

$$G = F_n + K_2^0 q_0(\mathbf{n}\cdot(\boldsymbol{\nabla}\times\mathbf{n})), \tag{2}$$

where K_2^0, q_0 are the high-temperature, i.e., N^* phase, twist elastic constant and twist wave number, respectively (the latter thus is the wave number of the director rotation around the helical axis in the chiral nematic phase). This expression is analogous to the Gibbs potential of superconductors. From this equivalence, the decrease ΔT_{tr}^{mf} of the transition temperature can be obtained in the mean-field approximation:

$$(\Delta T_{tr}^{mf})^2 = T_c\frac{K_2^0 q_0^2}{\Delta C}, \tag{3}$$

where ΔC is the (mean-field) specific heat capacity jump. In the scaling regime the free energy of the smectic-*A* phase has the form ($t \equiv (T - T_c)/T_c$ is the reduced temperature)

$$G_A = -\frac{\epsilon_0}{2}|t|^{2-\alpha}, \tag{4}$$

with ϵ_0 setting the energy scale, while

$$G_{N*} = -\frac{1}{2}\frac{(K_2^0 q_0)^2}{K_2}, \tag{5}$$

with K_2 including all enhancements due to fluctuations, so near T_c it diverges as $K_2 = K_2^1|t|^{-\nu}$. A transition occurs when $G_A = G_{N*}$, so the transition temperature decrease ΔT_{tr}^{sc} in the scaling regime is (using $d\nu = 2 - \alpha$)

$$\Delta T_{tr}^{sc} = T_c|t_{tr}| = T_c\left(\frac{(K_2^0 q_0)^2}{K_2^1\epsilon_0}\right)^{1/[(d-1)\nu]} \tag{6}$$

(here $|t_{tr}|$ is the value of $|t|$ at the transition). The author further makes a crude numerical estimate of this decrease leading to an order of magnitude of $\Delta T_{tr}/T_{NA} \approx 10^{-3}$. Furthermore, the entropy change $\Delta S = S_{N*} - S_A$ at the chiral nematic to cholesteric transition can be obtained from Eq. (4) and (6), using $S = -T_c(\partial G/\partial t)_p$:

$$\Delta S = (2 - \alpha)T_c\frac{\epsilon_0}{2}|t_{tr}|^{1-\alpha} \propto \Delta T_{tr}^{1-\alpha}. \tag{7}$$

Inserting the value of $|t_{tr}|$ [see Eq. (6)] yields (for $d = 3$)

$$\Delta S \propto (q_0)^{[2/(d-1)\nu](1-\alpha)} \propto (q_0)^{(1-\alpha/\nu)}. \tag{8}$$

So a latent heat $\Delta H_L = T_{tr}\Delta S$ is present, meaning that this model predicts the N^*A transition to be first order.

B. The model of Benguigui

A Landau approach has also been proposed by Benguigui [12]. Here, the smectic-*A* to chiral nematic transition is governed by a free energy in terms of the smectic order parameter Ψ_0 and the angle θ between the director and an axis perpendicular to the helical (z) axis of the chiral nematic phase, which can be written as [12]

$$G = \int\left[\frac{A}{2}|\Psi_0|^2 + \frac{C}{4}|\Psi_0|^4 + \frac{K_2}{2}\left(\frac{d\theta}{dz} - q_0\right)^2\right]dV, \tag{9}$$

where q_0 is the wave vector of the director rotation in the chiral nematic phase, K_2 is the Frank elastic constant, and $C(>0)$ is a positive constant. The coefficient of the second-order term is written as $A = a_0(T - T^*)$ where $a_0 > 0$ and T^* are constants.

In the chiral nematic phase, the smectic order parameter $|\Psi_0|$ is equal to zero, and the free energy is

$$G_{N*} = \frac{K_2}{2}\left(\frac{d\theta}{dz} - q_0\right)^2, \tag{10}$$

which is minimized by $q_0 = d\theta/dz$, so it reduces to zero. In the smectic-*A* phase, there is no rotation of the director around a helical axis, so $d\theta/dz = 0$ in Eq. (9).

In the absence of the chiral term (i.e., when $q_0 = 0$) we obtain an expression for a continuous *NA* and transition thus $T^* = T_{NA}$ being the *NA* transition temperature. The minima $|\Psi_0|_{min}$ in the Gibbs free energy are

$$|\Psi_0|_{min}=\begin{cases}0 & \text{when} \quad A>0,\\ \sqrt{-\dfrac{A}{C}} & \text{when} \quad A\leqslant 0.\end{cases} \tag{11}$$

A phase transition between the smectic-*A* and the chiral nematic phase occurs when $G_{N*}=G_A$, thus at $A=-\sqrt{2K_2Cq_0^2}=a_0(T_{N*A}-T_{NA})$ and consequently

$$T_{N*A}=T_{NA}-\frac{\sqrt{2K_2Cq_0^2}}{a_0}. \tag{12}$$

This transition is first order, since there is a discontinuous jump in the order parameter at the transition temperature between

$$|\Psi_0|=0 \quad \text{and} \quad |\Psi_0|=\sqrt[4]{\frac{2K_2q_0^2}{C}}. \tag{13}$$

The entropy discontinuity ΔS_{N*A} at this transition can easily be calculated to be

$$\Delta S_{N*A}=S_{N*}-S_A=a_0\sqrt{\frac{K_2q_0^2}{2C}}. \tag{14}$$

C. Relation to experiments

What is most interesting about these theoretical results for the transition temperature and entropy discontinuities of the N^*A transition is that they can be related to the experimental data by considering the fact that the wave vector q_0 of the chiral nematic director rotation is related to the pitch p as $|q_0|=\pi/p$. When we consider a mixture of a nonchiral with a chiral compound, the pitch of this mixture is, to a good approximation, given by [16,17]

$$\frac{1}{p_{chiral+nonchiral}}=\frac{x_{chiral}}{p_{chiral}}, \tag{15}$$

where p_{chiral} is the pitch of the (pure) chiral compound and x_{chiral} is the molar fraction of the chiral compound. This provides a means of relating the theoretical predictions of the previous sections to the experimental results obtained from such mixtures, since $|q_0|$ is proportional to x_{chiral}.

Thus, the results of Lubensky in the mean-field approximation [Eq. (3)] may be written as

$$\Delta T_{tr}^{mf}\propto x_{chiral}. \tag{16}$$

Using $d\nu=2-\alpha$ for $d=3$, in the scaling regime [Eqs. (6) and (8)] one obtains

$$\Delta T_{tr}^{sc}\propto(x_{chiral})^{3/(2-\alpha)}, \tag{17}$$

$$\Delta S\propto(x_{chiral})^{3(1-\alpha)/(2-\alpha)}. \tag{18}$$

Also, the predictions of Benguigui [Eqs. (12) and (14)] can be rewritten as

$$T_{N*A}=T_{NA}-Dx_{chiral}, \tag{19}$$

$$\Delta S_{N*A}=Ex_{chiral}, \tag{20}$$

with

$$D=a_0\sqrt{\frac{K_2}{2C}}\frac{\pi}{p_{chiral}} \quad \text{and} \quad E=\frac{\sqrt{2K_2C}}{a_0}\frac{\pi}{p_{chiral}}.$$

III. EXPERIMENT

A. Adiabatic scanning calorimetry (ASC)

The setup used for the measurements presented herein is an adiabatic scanning calorimeter consisting of four stages. The inner stage consists of the sample enclosed in a holder, which is surrounded by two concentric temperature-controlled shields (stages 2 and 3). The whole is enclosed in a third shield (stage 4) placed inside a hot air oven. The stability of this oven is about 1 K. However, excellent stability may be ensured inside: temperature fluctuations of stage 3 can be controlled to ± 2 mK and the difference between cell and the inner shield (stage 2) can be kept within ± 0.2 mK. This calorimeter can be used to carry out heating and cooling runs at very slow scanning rates, down to 1 mK/min, ensuring thermodynamic equilibrium. When applying a known constant heating (cooling) power P to the inner stage, the experimental curve of temperature versus time, $T(t)$, provides a direct measurement of the enthalpy change

$$H(T)-H(T_s)=\int_{T_s}^{T_{tr}}C\,dT+\Delta H_L+\int_{T_{tr}}^{T}C\,dT \tag{21}$$

$$=P(t_i-t_s)+P(t_f-t_i)+P(t-t_f), \tag{22}$$

where the index s refers to the starting conditions. This feature is unique to an ASC. Upon the occurrence of a first-order transition, the sample temperature will remain essentially constant at the transition temperature T_{tr} during a finite time interval $t_f-t_i=\Delta H_L/P$ where ΔH_L is the latent heat. For a continuous (second-order) transition, $\Delta H_L=0$. One should distinguish between the actual latent heat ΔH_L (i.e., the enthalpy jump at a first-order transition) and the pretransitional enthalpy increases, whereas the total transition heat is the sum of both. One must also note that, in practice, first-order transitions usually have a two-phase coexistence region, due to impurities or inhomogenitities in the sample. This results in a broadening of the latent heat jump over a (small) temperature interval. The heat capacity C_p of the inner stage is the sum of that of the holder, C_h, and the sample, C_s:

$$C_p=C_s+C_h=\frac{P}{\dot{T}}, \tag{23}$$

where $\dot{T}=dT/dt$ is obtained by numerical differentiation of the $T(t)$ data. The specific heat capacity of the sample is thus calculated by simply subtracting the holder contribution, which is measured in a separate experiment, and by dividing by the sample mass. This technique has already been employed for the study of a wide variety of phase transitions in

TABLE I. Details of the investigated 8OCB + CB15 samples (in order of preparation).

wt.%	x_{CB15}	m_{sample} (mg)
0	0	658.0
5.4	0.066	1831.4
10.2	0.12	1929.3
7.0	0.085	1922.0
11.9	0.14	1741.6
16.0	0.19	1827.8
19.0	0.22	1895.8
0.8	0.01	1807.2
3.6	0.044	1685.6
8.6	0.10	1779.4
2.7	0.033	2048.5
4.1	0.050	2077.1
5.8	0.071	1959.0
8.3	0.10	2007.0
13.8	0.17	1800.0
0	0	3922.4
0.74	0.0092	3922.1
1.8	0.022	3962.7

pure or in mixtures of liquid crystals [18–21], liquid crystal-aerosil mixtures [22], and other systems [23–25]. The ASC technique is described in more detail in Refs. [26,27].

B. Properties of the investigated samples

The nonchiral 8OCB is a member of the cyanobiphenyl family of homolog. Pure 8OCB has a phase sequence Cr-Sm*A*-*N*-*I*, having a nematic width of about 13 K. The chiral CB15 can be undercooled into the cholesteric phase. Its melting point lies around 4°C. Both compounds were obtained from Merck.

A study empolying optical polarization microscopy and DSC by Hwang *et al.* [15] reveals that mixtures of these compounds exhibit a phase sequence Cr-Sm*A*-*N**-*I*, where the chiral nematic width gets larger upon increasing CB15 fraction. Unfortunately, the width of the Sm*A* region was found to diminish with increasing CB15 fraction, until it was reported to vanish at a concentration of about 25 wt.% of CB15 where a crystalline to chiral nematic transition remains. Moreover, it is claimed in this paper that a TGB-like phase is present between the Sm*A* and *N** phases, based on a polarization microscopic investigation. At concentrations of more than 40 wt.%, blue phases were observed between the chiral nematic and the isotropic phases.

Mixtures were prepared inside the sample holder, by keeping its contents well above the *NI* transition temperature of 8OCB so that both compounds are in the isotropic phase while stirring for a period of approximately 1 h. In this manner, a homogeneous mixture of both components is obtained. All investigated mixtures were prepared according to this procedure (see Table I). In order to achieve better resolution in the low CB15 concentration region, where small latent heats are expected, one pure 8OCB sample and two low CB15 concentration mixtures were prepared inside a larger cell, which can contain approximately 4 g of liquid-crystal sample.

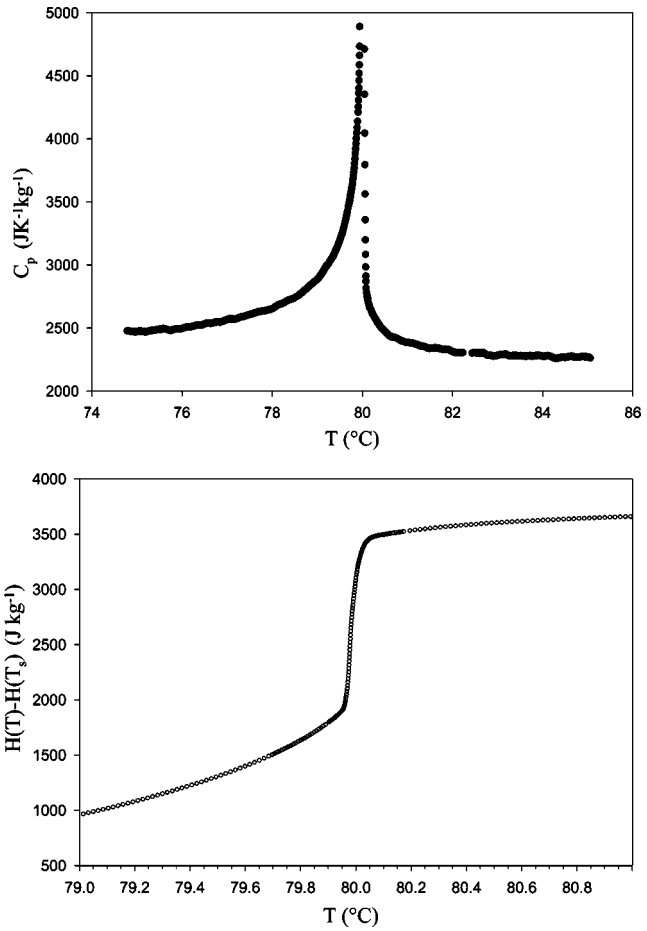

FIG. 1. Specific heat capacity and enthalpy change near the *NI* transition in pure 8OCB.

IV. RESULTS FOR PURE 8OCB

In view of the discussion surrounding the nature of the *NA* transition, we have conducted a close investigation of pure 8OCB. A preliminary study on a rather small quantity (658 mg) of 8OCB already showed that a possible latent heat would be quite small: an upper bound of 5 J/kg was established. The transition temperature was determined to be $T_{NA}=66.913$°C. The *NI* transition was clearly first order with a latent heat of 1540 ± 50 J/kg. A two-phase coexistence region of 0.09 K was present, extending from 79.95°C to $T=80.04$°C. The specific heat capacity and enthalpy change near this transition are plotted in Fig. 1. When comparing to literature values of $T_{NA}=67.12$ and $T_{NI}=80.2$ [14], a downwards temperature shift of 0.21 K for the *NA* transition and of 0.2 K for the *NI* transition is observed for this sample, the values of which are consistent with one another.

A more detailed experiment was performed where a relatively large quantity of 3.922 g of pure 8OCB was studied, since this allows detection of smaller latent heats. An overview of the specific heat capacity of this sample can be found in Fig. 2. Based upon specific heat capacity data of this pure

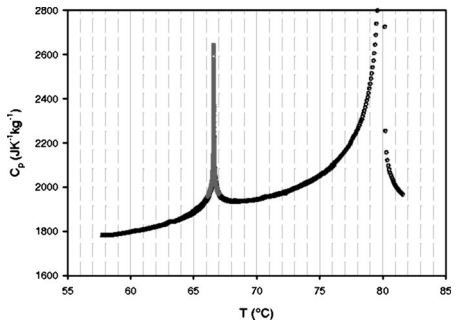

FIG. 2. An overview of the specific heat capacity of pure 8OCB.

8OCB sample, one may locate T_{NA} between 66.5925 and 66.5940 °C: a detail plot of the *NA* heat capacity shows some rounding of the $C_p(T)$ curve between these temperatures (see Fig. 3).

An additional method to distinguish between the first order and the continuous behavior is based on the quantity *C*, defined as

$$C=\frac{H-H_c}{T-T_c}, \tag{24}$$

H, H_c being the enthalpy at the temperature T and the critical temperature T_c, respectively. If the specific heat capacity C_p is of the form

$$C_p=A^{\pm}|t|^{-\alpha}+B, \tag{25}$$

with $t=(T-T_c)/T_c$, $A^{\pm}$ is the critical amplitude above and below T_c, α is the critical exponent, and B in the background term, it can be shown that

$$C-C_p=\frac{A^{\pm}}{1-\alpha}|t|^{-\alpha}, \tag{26}$$

so a log-log plot of $C-C_p$ versus t shows linear behavior with slope $-\alpha$ for a continuous transition. When, however, a value for T_c different from the actual critical temperature is used to calculate *C*, deviations from this linear behavior occur. This provides a means to check the location of the transition temperature (this is illustrated in Fig. 4 for three different choices of T_c).

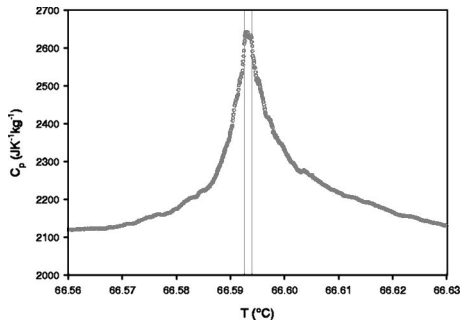

FIG. 3. Detail of the specific heat capacity of pure 8OCB near the *NA* transition.

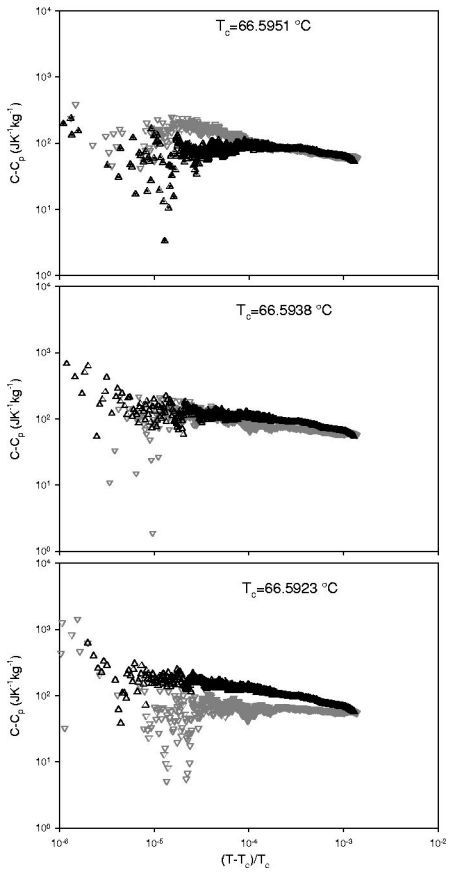

FIG. 4. Plot of the quantity $C-C_p$ vs the reduced temperature $t=(T-T_c)/T_c$ for different choices of T_c. Clearly $T_c=66.5938$ °C yields linear behavior both for $T>T_c$ and for $T<T_c$; so this is an appropriate value for the transition temperature. In contrast, the $T_c=66.5923$ °C and $T_c=66.5951$ °C curves differ from this behavior, thus showing that the actual transition temperature is different from these temperatures. See text for further details.

Upon close examination of the $C-C_p$ versus t curves for different choices of T_c, one can establish that T_c is not lower than 66.5927 °C and not higher than 66.5946 °C. Therefore we arrive at an upper boundary of a two-phase region (if any) of 2 mK, located at 66.5937 ± 0.001 °C. The corresponding upper bound for the latent heat, being the enthaply increase corresponding to the upper bound for the two-phase region, is $\Delta H_L^{max}=1.8$ J/kg. The difference in transition temperature between the high mass and low mass sample is probably related to the fact that a sample of a different batch of 8OCB was used. Moreover, a shift of the thermometers used may also play a role, especially when considering the long time between the two experiments (the low mass experiment was performed nearly 3 yr before the high-mass experiment) and the fact that a different sample holder (with a different thermometer) was used.

V. RESULTS FOR MIXTURES OF 8OCB AND CB15

A. Transition temperatures

Because the width of the chiral nematic region is of importance to the results, a heating run was performed to also

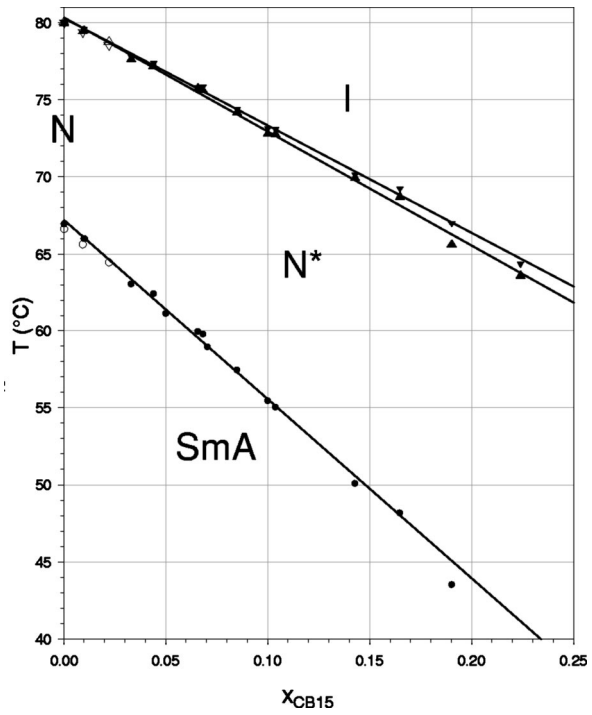

FIG. 5. Phase diagram of 8OCB + CB15 mixtures as obtained by an ASC. For the smectic-*A* to chiral nematic (N^*A) transition only the peak temperatures are plotted (dots), since the two-phase regions of these transitions are very small. For the chiral nematic to isotropic (N^*I) transition, the beginning and end of the coexistence region are plotted (triangles). Full lines represent linear fits through these points. Open symbols are data from three high-mass experiments (see text for further details).

determine the location of the NI transition for each mixture (except for $x_{CB15}=0.050$). Beginning and end of the N^*+I coexistence region are plotted in Fig. 5 confirming an increasing chiral nematic width upon increasing chiral (CB15) fraction. It is interesting to notice that these temperatures decrease linearly with the chiral fraction x_{CB15}. Moreover, the two-phase coexistence region of this first order N^*I transition widens with increasing chiral fraction.

Figure 5 also reveals that the N^*A transition temperatures decrease linearly with x_{CB15}. Only peak temperatures [i.e., temperatures of the maximum of the $C_p(T)$ peak] are shown, which is justifiable in view of the very small N^*+Sm*A* coexistence regions (see further). This corresponds to the prediction of Benguigui [see Eq. (19)] [12] as well as to the prediction derived by Lubensky in the mean-field approximation from an analogy with superconductors [Eq. (16)] [11]. A linear fit through the obtained values yields an intercept with the temperature axis of 67.2 ± 0.2 °C, close to $T_{NA}=66.913$ and a slope of -116 ± 2 K. From this fit, the data point at $x_{CB15}=0.19$ was omitted, which probably suffers from an error in the determined CB15 weight fraction. It must be noted that the transition temperatures of the three high-mass experiments (indicated by open symbols in Fig. 5) are not considered in this analysis. It can be observed that these samples tend to have a slightly lower N^*A transition temperature. As discussed in the preceding section, this is probably related to the use of 8OCB from a different batch.

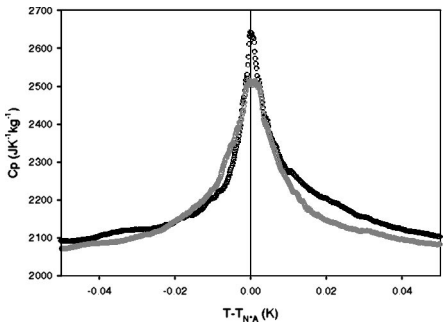

FIG. 6. Detail of the specific heat capacity of pure 8OCB (black) and the mixture with the lowest examined chiral fraction $x_{CB15}=0.0092$ (gray) as a function of $T-T_{N*A}$. The NA transition in pure 8OCB is found to be continuous within the experimental resolution. The N^*A transition in the mixture has an observable latent heat, as is noticable from the broadening near the transition temperature.

With Eq. (17), a literature value of the effective critical exponent $\alpha=0.27$ [13] suggests that $T_{NA}-T_{N*A}\propto(x_{CB15})^{1.7}$. Such an almost quadratic decrease of T_{N*A} does not correspond to the experiment. This exponent 1.7 must be considered an upper limit, since it is known for the NA transition that this critical exponent α decreases with decreasing McMillan ratio T_{NA}/T_{NI}, i.e., with increasing nematic width (see Fig. 19 in Ref. [18]). However, even if a crossover effect would occur for the N^*A transition and the critical exponent decreases to the XY model ($d=3,n=3$), value of $\alpha_{XY}=-0.007$, this would still give a dependence $T_{NA}-T_{N*A}\propto(x_{CB15})^{1.5}$ not in agreement with the experimental values.

It must be noted that a previous ac calorimetric examination of a system consisting of nonchiral octylcyanobiphenyl (8CB) liquid crystal with equal amounts of chiral CB15 and 4″-(2-methylbutylphenyl)-4′-(2-methylbuthyl)-4-biphenyl carboxylate (CE2) already revealed that $T_{N*I}-T_{N*A}$ increases linearly with the molar fraction of the chiral compound for four mixtures investigated between a chiral weight fraction of 0 up to 28% [17]. In our study, we have used results on 14 concentrations, up to $x_{CB15}=0.19$ (16 wt.%). At higher concentrations of CB15, the Sm*A* phase is no longer present (a direct transition from the crystalline to the chiral nematic phase was present at $x_{CB15}=0.22$), limiting our investigation to the previously mentioned concentration interval.

B. Enthalpy and latent heats

The result from our ASC investigation is that, for all investigated 8OCB + CB15 mixtures, a latent heat was observed, so that these N^*A transitions are first order (see Figs. 6 and 7). Since the chiral nematic width is larger for mixtures than for pure 8OCB and the latter has a (within experimental resolutions) continuous transition, one can conclude that the first-order character of these N^*A transitions is related to the effect of the presence of chirality in these mixtures, ruling out the possibility of a continuous to first-order crossover effect similar to that of the smectic-*A* to nematic transition. This is a direct confirmation of the first order character of the

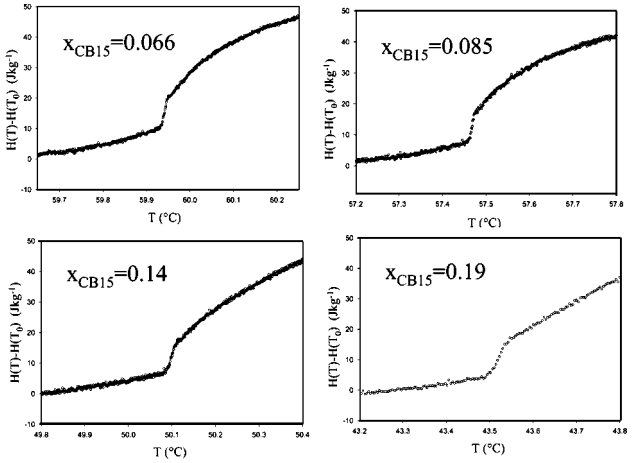

FIG. 7. Enthalpy change near the N^*A transition in the mixtures of 8OCB and CB15.

N^*A transition, as was predicted in Refs. [11] and [12]. Even though qualitatively these predictions are correct, quantitatively they do not agree with our experimental results. The evolution of the N^*A entropy discontinuities ΔS_{N^*A} with increasing chiral fraction (see Fig. 8) is not linear, as was suggested in Ref. [12]. In contrast, it seems that there is a relatively sudden increase at (very) low chiral fractions, followed by a more gradual evolution for higher CB15 concentrations. Unfortunately, the evolution at concentrations above $x_{CB15} \approx 0.20$ could not be investigated due to the fact that the Sm*A* phase vanishes between $x_{CB15}=0.19$ and $x_{CB15}=0.22$ (0.16 and 0.19 wt.%). Insertion of the value $\alpha=0.27$ [13] into the prediction of Lubensky [11] [see Eq. (18)] yields

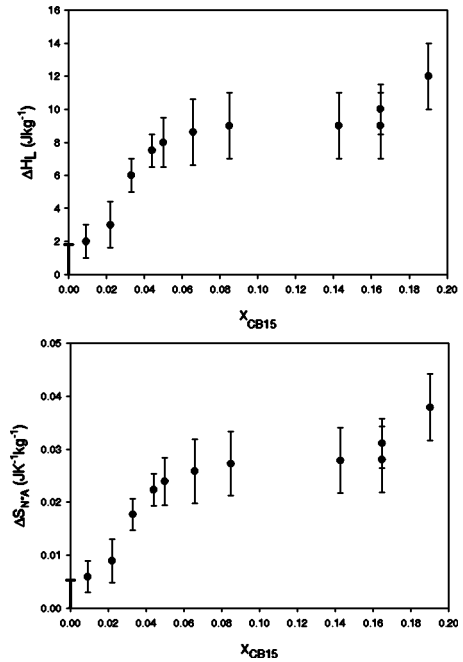

FIG. 8. Evolution of the latent heat and the entropy discontinuities of the N^*A transition in 8OCB+CB15 as a function of the chiral fraction x_{CB15}. For pure 8OCB only the upper bound for ΔH_L and ΔS_{N*A} is given.

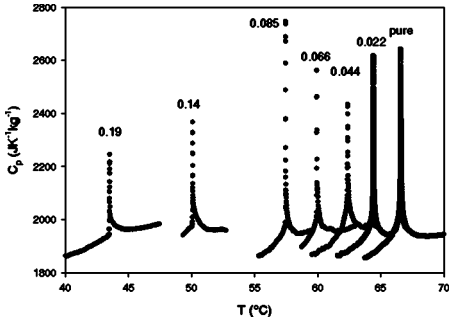

FIG. 9. Evolution of the specific heat capacity near the N^*A transition in mixtures of 8OCB+CB15. The chiral fraction x_{CB15} of the mixture is indicated above each $C_p(T)$ peak.

$\Delta S_{N*A} \propto (x_{CB15})^{1.3}$. This must be considered as a lower limit: if the critical exponent α were to diminish with increasing chiral nematic width to a value of $\alpha_{XY}=-0.007$, this would yield a dependence of $\Delta S_{N*A} \propto (x_{CB15})^{1.5}$. However, if ΔS_{N*A} were to be proportional to a power of the chiral fraction, experimental values suggest that this would be a power less than 1, so also this model does not give a good quantitative agreement.

It must also be noted that for all investigated mixtures, no additional phase was present between the smectic-*A* and the chiral nematic phases, in contrast to the claims emerging from an optical polarization microscopy study of Ref. [15], of the presence of a TGB-like phase between the Sm*A* and N^* phases. One might speculate that a texture at the coexistence of the Sm*A* and the N^* phase, which occurs since the N^*A transition is first order, was misinterpreted.

C. Pretransitional specific heat capacity

An overview of the specific heat capacity of the mixtures near the N^*A transition is given in Fig. 9. The pretransitional specific heat capacity of the N^*A transitions shows a very interesting evolution as a function of increasing chiral fraction. In order to clarify this, Fig. 10 shows the plots of Fig. 9 after subtraction of a linear $C_p(T)$ contribution and with the transition temperatures shifted to zero. For reasons of clarity the different curves were further shifted over multiples of 1 K and 100 $\mathrm{J\,K^{-1}\,kg^{-1}}$. It can be observed that first, the low-temperature side of the pretransitional specific heat capacity clearly becomes suppressed with increasing chiral fraction. Its high-temperature counterpart is not affected as much by a change in composition of the mixture, but at the highest CB15 concentrations one can observe that the pretransition at the high-temperature side becomes suppressed as well. The significance of this unusual phenomenon is not clear, and no account for this behavior is given in the theoretical approaches to the N^*A transition, which we discussed earlier. Clearly, a normal Landau theory description is not sufficient, since such an approach yields a zero excess specific heat capacity in the high-temperature phase. At high CB15 concentration one rather observes a rather unusual (inverted Landau type) behavior.

VI. CONCLUSION

The evolution of the smectic-*A* to chiral nematic (N^*A) transition in mixtures of the nonchiral liquid crystal 8OCB

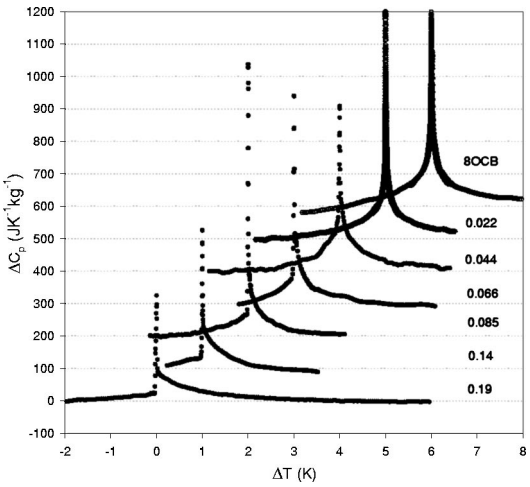

FIG. 10. Evolution of the pretransitional specific heat capacity near the N^*A transition in mixtures of 8OCB+CB15. The chiral fraction x_{CB15} of the mixture is indicated next to each curve. See text for further details and discussion.

and the chiral CB15 was studied by using an ASC. It was confirmed that, within experimental resolution, pure 8OCB exhibits a continuous *NA* transition in agreement with literature [14,13]. An upper limit for the latent heat is established at 1.8 $\mathrm{J\,kg^{-1}}$. Mixtures with CB15 exhibit a phase sequence Cr-Sm*A*-N^*-I with an increasing chiral nematic width [15], until the Sm*A* phase vanishes between $x_{CB15}=0.19$ and $x_{CB15}=0.22$. This rules out crossover behavior from a continuous to a first-order transition as is the case for the smectic-*A* to nematic transition if the nematic width is small enough [5,6].

Theoretical predictions of the first order character of this transition [11,12] were confirmed by the fact that for all examined mixtures a latent heat could be determined. Because of the increasing chiral nematic width, the possibility of a crossover effect prediction for the (normal) *NA* transition can be ruled out. It was further observed that the N^*A transition temperature decreases linearly with temperature according to the theoretical predictions of Benguigui [12] and to the results derived by Lubensky from an analogy with superconductors in the mean-field approximation [11], and also confirming the observation of a previous study [17]. However, quantitative predictions of Lubensky and Benguigui for the evolution of the entropy discontinuity and the latent heat at this transition did not agree with the experimental values.

Moreover, a very interesting behavior of the $C_p(T)$ pretransition was observed. Upon increasing chiral fraction, the low-temperature side became clearly suppressed. Additionally, also some depression of the high-temperature specific heat capacity wing is visible at high CB15 concentrations. Thus, the $C_p(T)$ peak near the N^*A transition becomes more asymmetric in shape when the chiral fraction increases. This kind of behavior is not included in the current theoretical descriptions [11,12]. The reasons for its occurrence are not as yet clear.

Finally, the *NI* transition of pure 8OCB was found to be clearly first order, with a latent heat $\Delta H_L=1540\pm50\ \mathrm{J\,kg^{-1}}$ and a two-phase coexistence region located between $T=79.95\,^{\circ}\mathrm{C}$ and $T=80.04\,^{\circ}\mathrm{C}$.

ACKNOWLEDGMENTS

This work was supported by the Fund for Scientific Research Flanders (Belgium) (FWO, Project No. G.0264.97N and G.0246.02). P. J. gratefully acknowledges financial support from the Research Council of the KU Leuven.

[1] P.G. de Gennes, Solid State Commun. **10**, 753 (1972).
[2] G. Vertogen and W.H. de Jeu, *Thermotropic Liquid Crystals, Fundamentals* (Springer-Verlag, Berlin, 1988).
[3] C.W. Garland and G. Nounesis, Phys. Rev. E **49**, 2964 (1994).
[4] P.G. de Gennes and J. Prost, *The Physics of Liquid Crystals*, 2nd ed. (Clarendon, Oxford, 1993).
[5] J. Thoen, H. Marynissen, and W.V. Dael, Phys. Rev. Lett. **52**, 204 (1984).
[6] H. Marynissen, J. Thoen, and W.V. Dael, Mol. Cryst. Liq. Cryst. **124**, 195 (1985).
[7] B.I. Halperin, T.C. Lubensky, and S.K. Ma, Phys. Rev. Lett. **32**, 292 (1974).
[8] A. Yethiraj and J. Bechhoefer, Phys. Rev. Lett. **84**, 3642 (2000).
[9] C.W. Garland, Liq. Cryst. **26**, 669 (1999).
[10] H. Stegemeyer, T.H. Blmel, K. Hiltrop, H. Onusseit, and F. Porsch, Liq. Cryst. **1**, 3 (1986).
[11] T.C. Lubensky, J. Phys. C **1**, 151 (1975).
[12] L. Benguigui, Liq. Cryst. **25**, 505 (1998).
[13] G.B. Kasting, K.J. Lushington, and C.W. Garland, Phys. Rev. B **22**, 321 (1980).
[14] C.W. Garland, G.B. Kasting, and K.J. Lushington, Phys. Rev. Lett. **43**, 1420 (1979).
[15] J.C. Hwang, S.C. Liang, K.H. Liang, and J.R. Chang, Liq. Cryst. **26**, 925 (1999).
[16] D.K. Yang and P.P. Crooker, Phys. Rev. A **35**, 4419 (1987).
[17] G.S. Iannachione, S. Qian, M. Wittebrood, and D. Finotello, Mol. Cryst. Liq. Cryst. **302**, 1 (1997).
[18] J. Thoen, Int. J. Mod. Phys. B **9**, 2157 (1995).
[19] J. Thoen, H. Marynissen, and W.V. Dael, Phys. Rev. A **26**, 2886 (1982).
[20] M. Young, G. Pitsi, M.-H. Li, H.-T. Nguyen, P. Jamée, G. Sigaud, and J. Thoen, Liq. Cryst. **25**, 387 (1998).
[21] P. Jamée, G. Pitsi, M.-H. Li, H.-T. Nguyen, G. Sigaud, and J. Thoen, Phys. Rev. E **62**, 3687 (2000).
[22] P. Jamée, G. Pitsi, and J. Thoen, Phys. Rev. E **66**, 021707 (2002).
[23] A. Cruz-Orea, G. Pitsi, P. Jamée, and J. Thoen, J. Agric. Food Chem. **50**, 1335 (2002).
[24] A. Cruz-Orea, E.H. Bentefour, P. Jamée, M. Chirtoc, C. Glorieux, G. Pitsi, and J. Thoen, Rev. Sci. Instrum. (to be published).

[25] G. Pitsi, J. Caerels, and J. Thoen, Phys. Rev. B **55**, 915 (1997).
[26] J. Thoen, in *Physical Properties of Liquid Crystals*, edited by D. Demus, J. Goodby, G. Gray, H.-W. Spiess, and V. Vill (Wiley-VCH, Weinheim, 1997), pp. 208–232.
[27] J. Thoen, E. Bloemen, H. Marynissen, and W.V. Dael, in *Proceedings of the 8th Symposium on Thermophysical Properties, National Bureau of Standards, Maryland 1981*, edited by J.V. Sengers (American Society of Mechanical Engineers, New York, 1982), pp. 422–428.